Jordan Journal of Civil Engineering, Volume **15**, No. **1**, **2021**

Ultimate Load Response of a Square Footing Subjected to Axial and Eccentric Load on Geogrid-Reinforced Soil

Anand Shrigondekar [1)*] ***and Prabhuling Ullagaddi*** [2)]

[1)] Research Scholar, Shri Guru Gobind Singhji Institute of Engineering and Technology, Nanded- 431606, Maharashtra State, India.
* Corresponding Author. E-Mail: anandshrigondekar7@gmail.com
[2)] Professor, Shri Guru Gobind Singhji Institute of Engineering and Technology, Nanded- 431606, Maharashtra State, India.

ABSTRACT

This research attempted to contemplate the conduct of experiments on reinforced sand in enhancing the bearing capacity of a square footing. Locally available river sand along with geogrid as a reinforcement material were utilized. The experiments were completed in an M.S. tank of size 0.75m x 0.75m x 0.75m. A plate vibrator was used to compact the soil and the vertical load was applied using a hydraulic cylinder of 50 kN capacity. In this study, a total of 104 tests were performed on a square footing with central load as well as for eccentric loading. The parameters considered in the exploratory investigation include the effect of the uppermost layer of geosynthetic on the load-carrying capacity of a footing, the number of layers of reinforcement sheets, eccentricity of loading and vertical spacing between successive layers. The experimental reading indicates that for a given geogrid-strengthened sand, the topmost layer of the geogrid was at 0.25 times the footing breadth from the base of the footing to achieve maximum load capacity, while the optimum spacing between successive geogrid layers was also found as 0.25 times the width of footing. It was confirmed that the Bearing Capacity Factor (BCF) reaches its highest value when 4 layers of geogrid are used in the soil and the load-carrying capacity of the footing is reduced by 20% to 40% when a load is applied at kern boundary.

KEYWORDS: Load intensity, Axial load, Eccentric load, Geogrid reinforced soil, Square footing, Unreinforced soil.

INTRODUCTION

The use of geosynthetic reinforcement has been widely accepted as the accessibility of reasonable construction sites diminishes and to meet expanding demand by using poor soil as a foundation material. The escalating use of geosynthetic reinforcement soil framework for significant structures requires legitimate comprehension of its conduct. The foundation soil being weak in tension, geosynthetic materials, such as geotextile, geocell, geomembrane and geogrid, are utilized to fortify poor soil, which leads to an enhancement in ultimate load capacity of the soil (Durga Prasad et al., 2016). The fundamental target of the soil strengthening technique is to develop stability, enhance load capacity and lessen settlements. In the ongoing decades, a few trial experiments have been completed to analyze the load-displacement study of various soil types (Marto et al., 2013). Soil fortification system shows that geosynthetic material gives horizontal and vertical confinement of soil, as well as more extensive stress distribution, as observed from Fig. 1. Few researchers have studied the area of geosynthetic soil reinforcement by considering various parameters. Deb & Konai (2014) varied the percentage of fines in sand from 5% to 30% and found that the geotextile was more effective for sand having 5% fines. Kodicherla et al. (2018) studied the effect of randomly distributed fiber reinforcement by considering beach sand as a soil medium. The outcome of the test indicated that the inclusion of fiber increases the frictional resistance, permeability and porosity values because of the absence of a potential barrier between solid particles in the

Received on 1/8/2020.
Accepted for Publication on 27/11/2020.

medium. By varying the depth and width of the geogrid, Alawaji (2001) found a maximum of 320% enhancement in load pressure and a 95% decrease in collapsible settlement. Makkar et al. (2017) used three-dimensional geogrids having rectangular and triangular openings to compare improvement factors in bearing capacity. For a rectangular opening and triangular opening, the improvement in BCF was observed as 3.05 and 2.7, respectively. Mittal and Shukla (2020) conducted soaked CBR and heavy compaction tests by using a geogrid placed in single and double layers from the top of the mould. It was noticed that CBR values increased 83% and 130% when the geogrid was placed in a single layer and for a double layer, respectively. Das & Omar (1994) studied the effect of the width of footing; the results obtained confirmed that the bearing capacity ratio of the geogrid-sand system reduces with increasing the breadth of footing. When the footing width was more than 130 mm to 140 mm, CBR reached a constant value. Sridhar and Prathapkumar (2017) computed the bearing capacity of sand using coir geotextile and the settlement reduction factor (SRF) was calculated for different d/B ratios. SRF increases with an increase in d/B ratio up to 0.8; afterwards, the increase in SRF was marginal. Aldaood et al. (2020) studied the impact of hay fiber on engineering properties of clayey soil. The percentage of hay fiber by weight was varied from 0.25% to 1.5%. As hay fiber content increases up to 1%, the strength parameter; i.e., unconfined compressive strength, increased and for a higher percentage of fiber, it was reduced. Durga Prasad et al.(2016) calculated load improvement factors for a geogrid-reinforced sand layer as 1.1 to 1.8 and for aggregate layer overlying sand by using geogrid, the values were 1.3 to 2.7, when the settlement ratio ranged from 5% to 15%. Tavangar and Shooshpasha (2016) carried out laboratory plate load tests by using 27cm x 27cm and 35cm x 35cm square plates. The maximum bearing pressure was found when the first layer of geotextile was placed at 0.2 B and 0.15 B for 27cm x 27cm and 35cm x 35cm plates, respectively. Dash et al. (2001) conducted experiments on strip footing using geocell. They discovered that in the presence of geocell, the ultimate load increased by 8 times that of unreinforced sand. It was also suggested that a chevron pattern was more beneficial than a diamond pattern. Patel and Singh (2017) conducted California Bearing Ratio tests on cohesive soil using fiber reinforcement to find the suitability of a sub-grade material. The CBR estimations of unreinforced soil for 4, 20 and 40 soaking days were 2.89, 2.54 and 2.33 and CBR values of soil with glass fiber fortification were 8.23, 6.24 and 5.03 for the respective soaking days. Panigrahi and Pradhan (2019) conducted experiments on geotextile-reinforced sand using natural gunny bags (geojute) as geotextile material. The extreme bearing capacity on strengthened soil was noticed as 3.37 times that of soil without geojute.

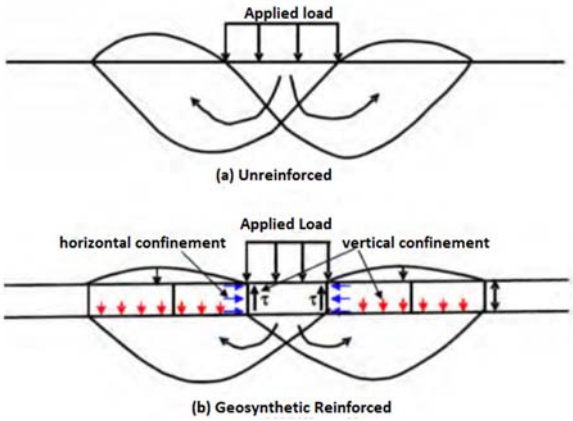

Figure (1): Unreinforced and reinforced soil behavior

Mirzaeifar, Zidan, Kolay and Dastpak studied the behavior of geosynthetic-reinforced soil by observing the effect of the shape of footing, load type (static or dynamic),…, etc. on the bearing capacity of the soil. A review of literature related to geosynthetic soil reinforcement shows that most of the laboratory/numerical studies concentrated on the various parameters of soil, the variation in geosynthetic material or the variation in footing dimensions. In the present research, a new type of biaxial geogrid (SB 30-30) was used throughout the testing as a reinforcement material and poorly graded sand was used as soil medium. In this paper, it is attempted to study the load-displacement behavior of square footing by considering the effect of individual parameters, such as the uppermost geogrid layer, the number of geosynthetic layers, the eccentricity of loading and the vertical spacing between two layers. Also, the optimum use of geosynthetic material for a given geogrid reinforcement system has been identified.

MATERIAL PROPERTIES

In this experimental study, two sorts of materials are utilized; i.e., sand and geogrid**.**

Sand

The soil utilized in the current study was dry sand, procured from Godavari River near Nanded (MH). The test sample was prepared by sieving through an appropriate sieve and the grading of sand particles was used as fine to medium size. Specific gravity, grain size distribution (GSD), maximum density and relative density were investigated and direct shear test was conducted on the test sample in accordance with IS 2720 relevant parts. According to the U.S. classification system, the test sample is classified as poorly graded sand and is denoted by SP. The properties of sand are listed in Table 1.

Table 1. Properties of sand

Property	Value
Specific gravity	2.614
D_{10} (mm)	0.4
D_{30} (mm)	0.48
D_{60} (mm)	0.87
Uniformity coefficient (C_u)	2.175
Coefficient of curvature (C_c)	0.662
Bulk density (kN/m^3)	16.58
Dry density (kN/m^3)	15.49
Angle of internal friction (ϕ)	36^o
Max. void ratio	0.9
Min. void ratio	0.48

Geogrid

The geogrid used in this investigation is of biaxial extruded polypropylene, fabricated by Strata India Private Limited Mumbai. The geogrid utilized is having a square aperture of 38mm size and is denoted by SB 30-30. 30 is the tensile strength of geogrid in kN/m in both cross-machine and machine directions. The mechanical and physical properties of geogrid were resolved according to ASTM D. The geogrid properties are enlisted in Table 2.

Table 2. Properties of Geogrid

Property	Specifications	
	Machine Direction (MD)	Cross-machine Direction (CMD)
Tensile strength (kN/m)	31.3	29.3
Tensile strength @ 2% elongation (kN/m)	14.2	14.9
Tensile strength @ 5% elongation (kN/m)	22.5	25.9
Maximum elongation (%)	13.8	7.52
Thickness (mm)	2.7	1.49
Mass (g/m^2)	293	
Single rib strength (N)	1188	
Junction strength (N)	1182	
Junction efficiency (%)	99.5	
Size of aperture (mm^2)	38 x 38	
Material	polypropylene	

METHODOLOGY

Laboratory Model Test

The trial set-up comprises a reaction frame, a mild steel tank, a hydraulic cylinder, a power pack, an electrical panel and a model footing. The actual experimental set-up utilized for the study is shown in Fig. 2. A reaction frame having a width of one meter and a height of 1.2m was installed. The width of the tank was prepared equal to 6.25 times the footing width to prevent the effect of boundaries. The front face of the tank was made up of an 18mm thick acrylic sheet to observe the failure surface and the remaining sides of the tank were prepared from mild steel of 8 mm thickness. Bracing was given along the side on the external face to abstain from yielding during the test. A model square footing of 120mm size and 25mm thickness was chosen, so that the width of footing is nearly equivalent to three times the opening size of the geogrid. The test footing base was prepared harsh by applying a slight layer of sand to it with an epoxy stick. A 50 kN pressure and 200mm stroke cylinder was provided applying load on balance. Pressure can be adjusted from zero to 250 bar using a power pack of 50 lit limits. The electric panel was provided on the right column of the frame for controlling up and down movement of the pressure cylinder.

Figure (2): Photograph of the test set-up

Sand Bed Preparation

The sand utilized in the investigation was passing through a 2mm sieve and held on a 75 micron sieve. Sand beds were prepared by using sand raining methodology and the height of fall was fixed as 300 mm from the top surface. The test tank was loaded up with sand of required consistent thickness in unreinforced as well as fortified sand. For reinforced sand, geogrids were inserted in the sand at required values of x/b and z/b. The filled surface was compacted by utilizing a vibrator.

Test Procedure

The test footing was placed on a prepared sand bed. A provision was made at the center of the footing and at 20mm from the center, to facilitate the application of loads on the footing. A proving ring of 50kN was placed at the center or at an eccentricity of 20 mm from the center of footing. Two dial gauges of 0.01 mm accuracy were located on the opposite edges of the footing to measure settlement values. Then, loads were applied in each small increment and the corresponding displacements were recorded. In this way, the entire load settlement plot was obtained for different sets of load and settlement values. The load increment was continued till it arrived at the ultimate load or extreme allowable settlement. The schematic diagram showing all parts of the test set-up is shown in Fig. 3.

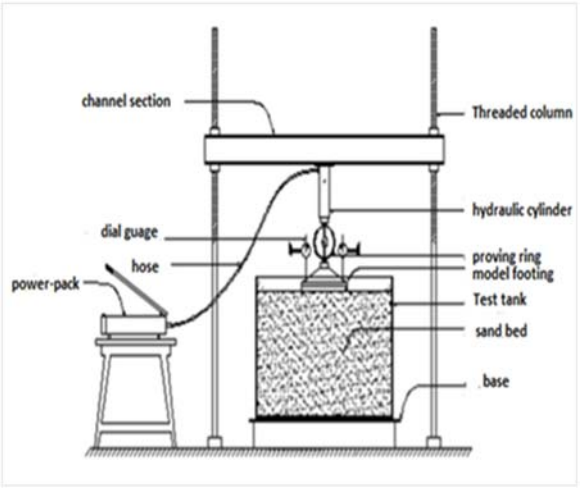

Figure (3): Schematic diagram of test set-up

Following notations are adopted in this study, as depicted in Fig.4.

b = footing width.

B = geogrid width.

N = number of geogrid layers.

x = distance of top layer of geogrid below the footing.

z = vertical distance between two successive layers of geogrid.

e = eccentricity (mm).

s = settlement (mm).

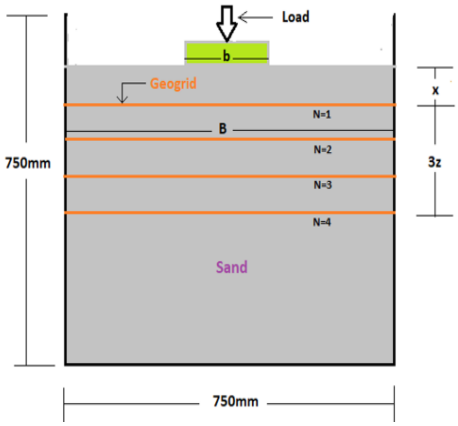

Figure (4): Layers of geogrid below the footing

RESULTS AND DISCUSSION

In this exploration, comparative studies have been made between the central load and eccentric load on a footing. The load settlement responses in each case have been computed. Experiments have been performed on 98 distinct combinations of geogrid position and the best reasonable arrangement of geogrid which achieves

maximum ultimate bearing capacity has been recommended. Also, improvement factors in bearing capacity due to provision of geogrid have been computed in each case, known as Bearing Capacity Factor (BCF). It is expressed as:

$$\text{BCF} = \frac{\text{Maximum load intensity of reinforced soil}}{\text{Maximum load intensity of unreinforced soil}}$$

An eccentric load is applied at a distance of 20 mm from the center of footing, because for a square footing of 120mm side, the kern boundary is b/6, which is 20mm. The kern of footing is the part of footing in which the whole footing is subjected to compressive pressure without producing tension on the cross-section. Hence, to avoid tension in the cross-section, eccentricity is limited to 20 mm. The effects of various parameters and variables used in the study are depicted in Table 3.

Table 3. Different variable parameters used in the test

Sr. no.	Test series	Variable parameters used in the study
1	Effect of first depth of reinforcement	$\frac{x}{b} = 0.25, 0.50, 0.75, 1.0$
2	Effect of spacing between reinforcements	$\frac{z}{b} = 0.25, 0.50, 0.75, 1.0$
3	Effect of number of layers of reinforcement	N = 2, 3, 4
4	Effect of position of load on the footing	e = 0, 20mm

The very first test performed in this research was without any reinforcement in soil. The graph of load intensity *versus* (s/b) % for unreinforced soil is plotted for centric load and eccentric load, as shown in Fig. 5.

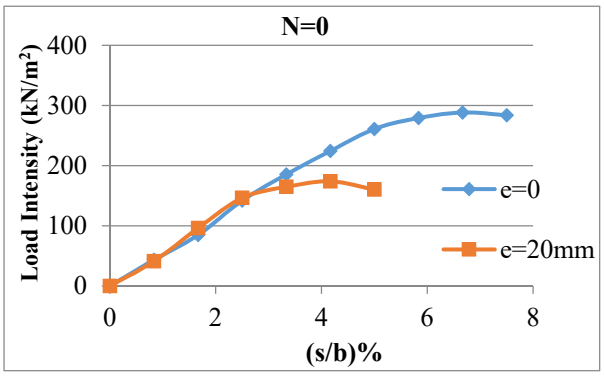

Figure (5): Load intensity *versus* % settlement for e = 0 and e=20 mm

When a load is applied on the footing, at the initial stage, the graphs of e=0 and e=20mm mostly coincide, but the values of ultimate load intensities are observed as 288.28 kN/m^2 and 173.88 kN/m^2 for e=0 and e=20mm, respectively. For unreinforced soil, when a load is applied at an eccentricity of 20mm, the maximum load beared by footing is nearly 39% less than that of load applied at the center. The remaining tests were carried out for reinforced soil by considering the parameters stated in Table 3. The geogrid used in this investigation is having a width of 3 times the width of footing, which is equal to 360mm. The geogrid depth was changed from 30mm to 120mm from the base of footing and the load settlement responses of strengthened soil in case of a single layer of geogrid were recorded for centric load and eccentric load, as shown in Fig.6a and Fig.6b, respectively.

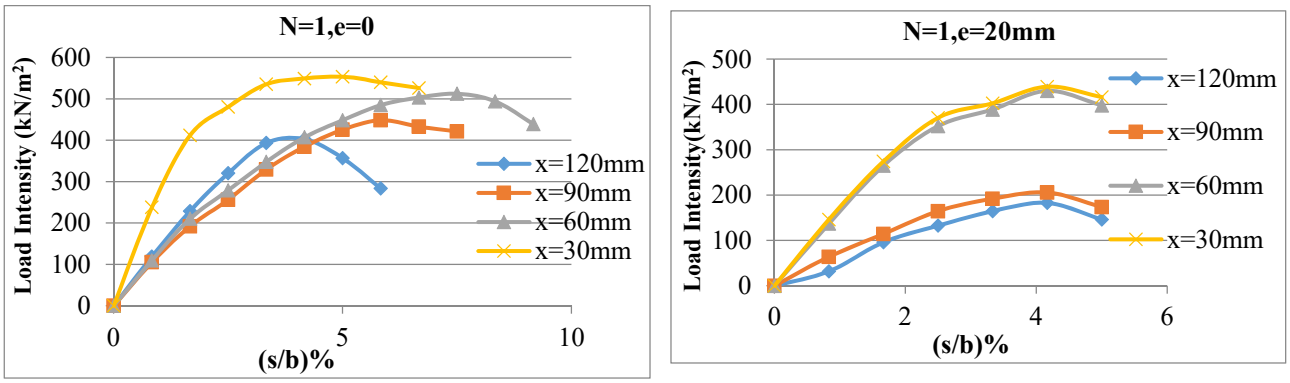

(a) **(b)**

Figure (6): Load intensity *versus* % settlement for single layer of geogrid (a) e=0 and (b) e = 20m

Effect of Depth of Reinforcement

The embedment depth of reinforcement sheets below the footing base is the most significant parameter in geosynthetic fortified soil. In this effort, the most advantageous depth of reinforcement in terms of the uppermost layer of geogrid and distance between successive layers has been determined. To find the optimum depth of geogrid, the top layer of geogrid varied from 30mm to 120mm (top depth ratio x/b as 0.25, 0.5, 0.75 and 1.0). The load-displacement response in each case was found out and it is noticed that for x/b= 0.25; i.e., the first layer of geogrid at 30mm from the footing base shows maximum ultimate pressure. Consequently, the diagrams are introduced for x=30mm in Fig. 7, Fig. 8 and Fig. 9 for two, three and four layers, separately.

Part 'a' represents the central load on the footing and part 'b' is for eccentric load at 20mm. The distinctive spacings between two layers of geogrid having depth ratio z/b = 0.25, 0.5, 0.75 and 1.0 were considered. The load settlement responses are observed in Fig. 7, Fig. 8 and Fig. 9 at the optimum depth of the first layer. From the outcomes, it is comprehended that the depth proportion z/b =0.25 gives the highest value of ultimate load intensity, for both e=0 and e=20mm.

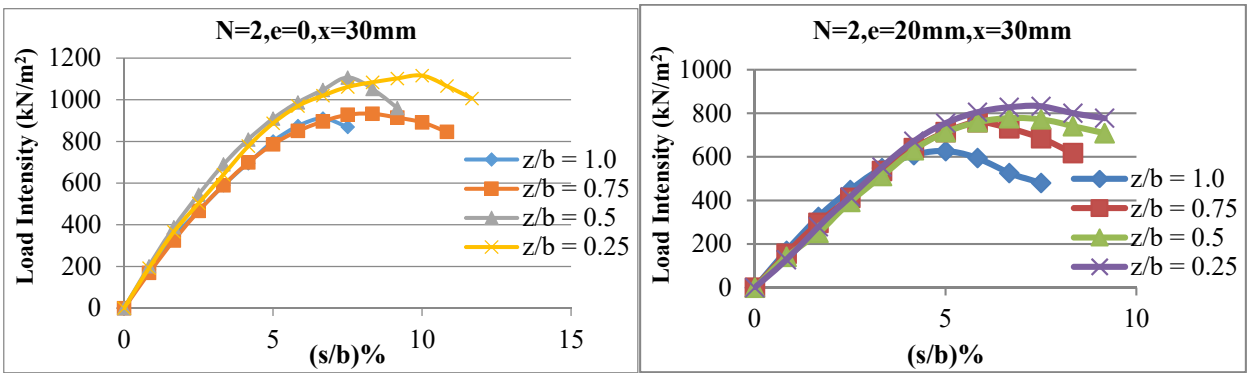

(a) **(b)**

Figure (7): Load settlement response for two layers of geogrid when the first layer is at 30mm (a) e=0 and (b) e=20mm

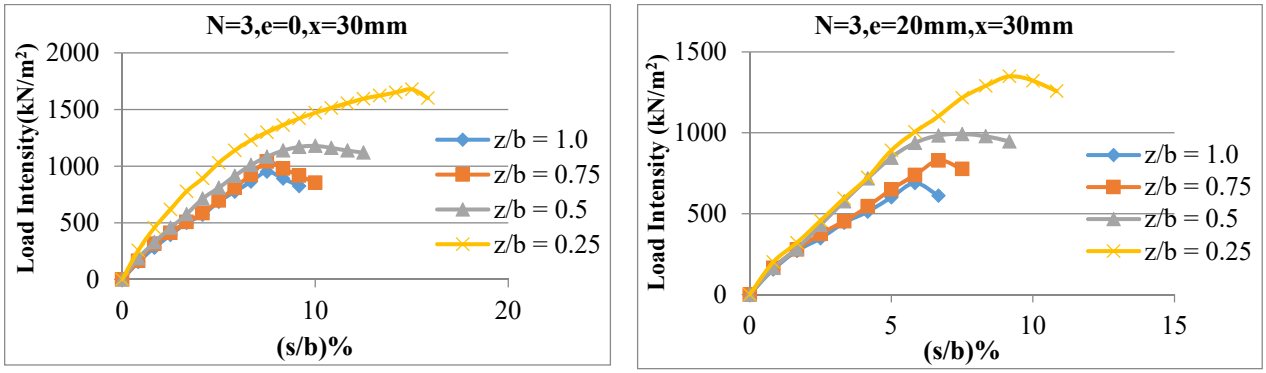

(a) **(b)**

Figure (8): Load settlement response for three layers of geogrid when the first layer is at 30mm (a) e=0 and (b) e=20mm

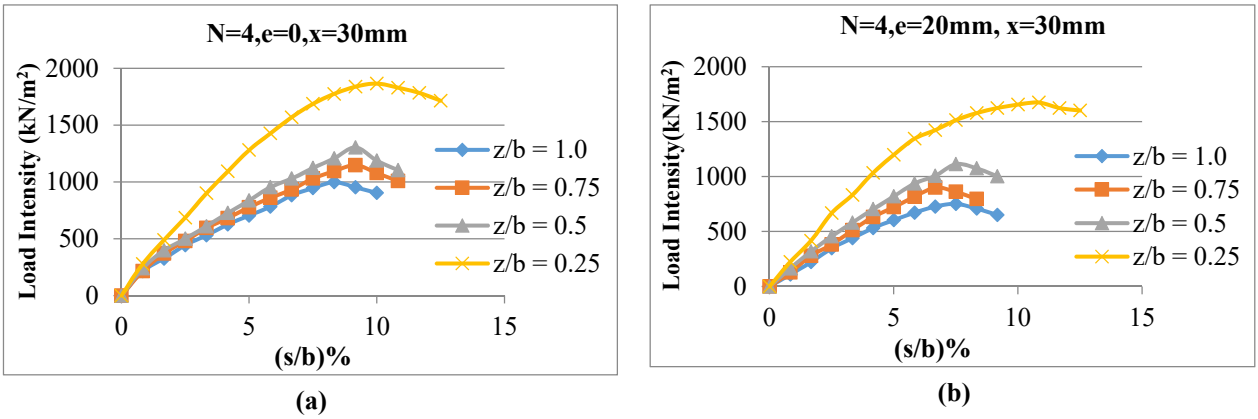

Figure (9): Load settlement response for four layers of geogrid when the first layer is at 30mm (a) e=0 and (b) e=20mm

Table 4. Ultimate load intensities for 2, 3 and 4 layers of geogrid when e=0

	Ultimate Load Intensities (kN/m²) for e=0											
	x=120mm			x=90mm			x=60mm			x=30mm		
	N=2	N=3	N=4	N=2	N=3	N=4	N=2	N=3	N=4	N=2	N=3	N=4
z/b = 1.0	411.8	475.8	501.36	516.4	626.9	736.72	668.0	704.6	827.38	910.6	952.0	998.24
z/b = 0.75	502.3	549.1	569.21	601.1	736.7	874.00	690.9	814.5	904.21	933.4	1040.9	1148.5
z/b = 0.50	549.1	567.4	620.35	669.6	759.6	910.61	901.4	1075.3	1210.854	1107.38	1180.6	1304.85
z/b = 0.25	571.99	654.36	709.2	822.64	906.03	1176.02	988.40	1194.3	1537.52	1116.53	1679.3	1866.99

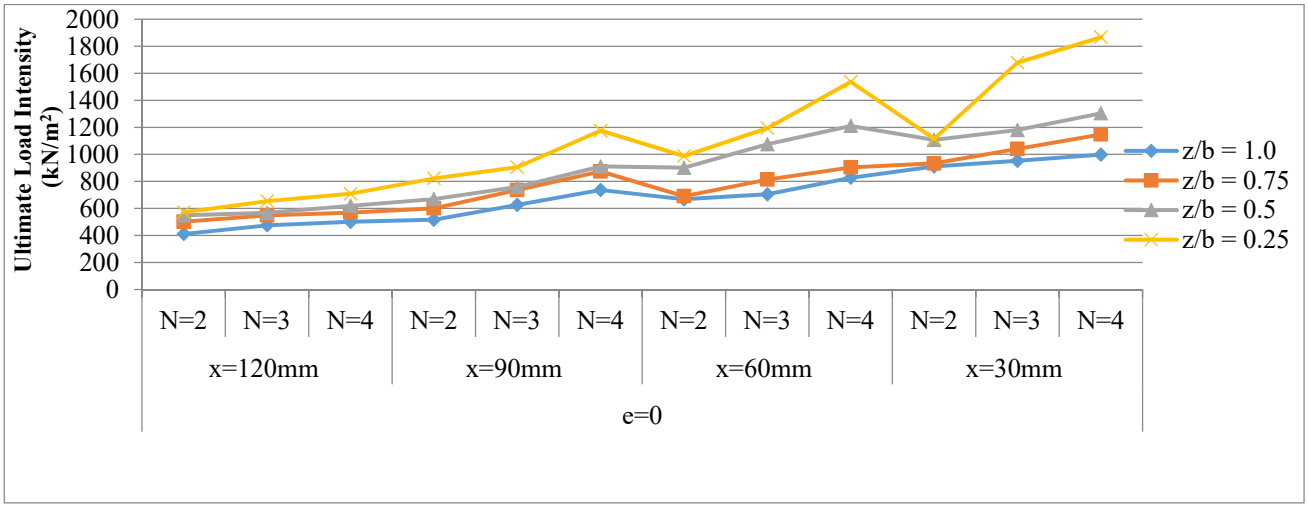

Figure (10): Ultimate load intensities for 2, 3 and 4 layers of geogrid when e=0

Effect of Number of Layers of Reinforcement

96 tests were performed for various depth ratios x/b and z/b to understand the impact of the number of layers of geogrid on the bearing capacity of centrally loaded and eccentrically loaded square footing. From load-displacement curves, the ultimate load intensities were recorded and are presented in Table 4 for e=0 and indicated graphically in Fig. 10. In each of the 4 cases; i.e., z/b=1.0, z/b=0.75, z/b=0.5 and z/b=0.25, Fig. 10 illustrates that the ultimate load intensity increases by adding layers from N=2 to N=4 and by decreasing x from 120mm to 30mm. In the same way, ultimate load intensities for 2, 3 and 4 layers of geogrid for e=20mm are given in Table 5 and plotted in Fig. 11. The results

of ultimate load intensity for e=20mm were observed in similar variation as those of e=0. When the number of layers increased from 2 to 3 and from 3 to 4, the average increment in bearing capacity was 15.44% and 13.69%, respectively, for e=0, while for eccentric load at 20mm, the average increment in bearing capacity was 22.97% and 14.95%, respectively.

Table 5. Ultimate load intensities for 2, 3 and 4 layers of geogrid when e=20mm

	Ultimate Load Intensities (kN/m²) for e=20mm											
	x=120mm			x=90mm			x=60mm			x=30mm		
	N=2	N=3	N=4	N=2	N=3	N=4	N=2	N=3	N=4	N=2	N=3	N=4
z/b = 1.0	256.25	393.53	412.02	321.47	462.17	485.05	424.46	485.05	603.52	626.906	689.24	751.247
z/b = 0.75	338.24	425.56	466.00	416.85	503.69	521.65	526.62	604.02	701.42	759.60	829.48	900.253
z/b = 0.50	391.65	448.36	528.36	520.52	591.14	753.14	622.33	741.30	812.68	773.33	992.98	1114.25
z/b = 0.25	512.50	560.86	618.65	604.02	685.32	804.026	672.63	773.33	1079.92	832.82	1349.9	1674.8

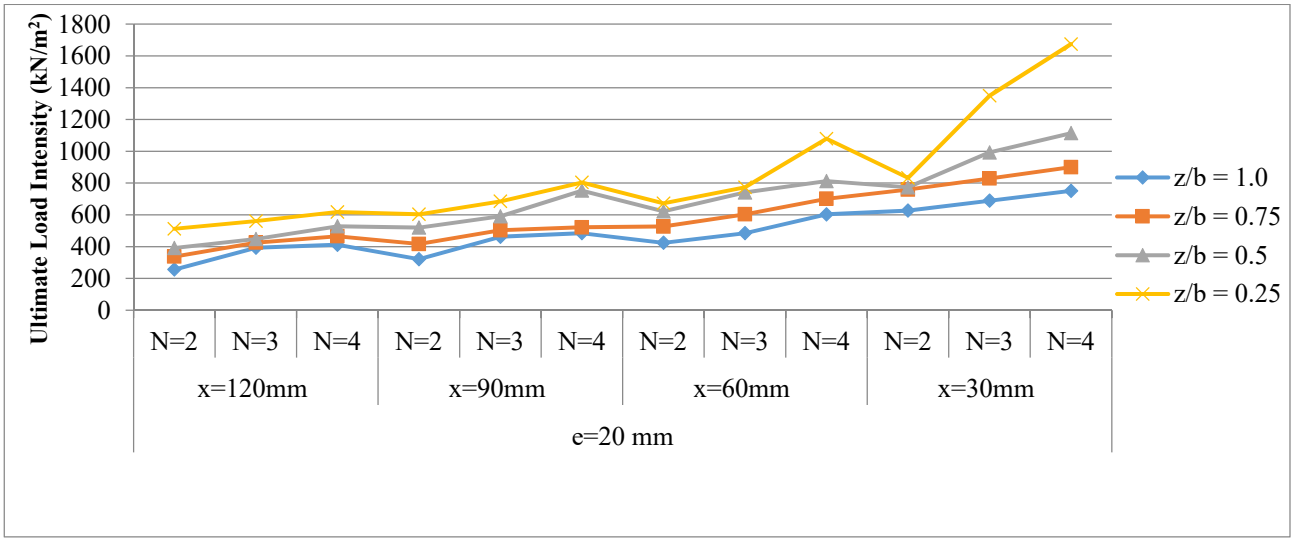

Figure (11): Ultimate load intensities for 2, 3 and 4 layers of geogrid when e=20mm

The effect of the number of layers is observed from Bearing Capacity Factor (BCF). Table 6 is introduced for BCF at e=0. The bar chart shown in Fig. 12 demonstrates that BCF was found to be increased when the number of layers increased from N=2 to N=4. The highest BCF is observed for 4 layers of geogrid, with z/b =0.25 and x= 30mm. Comparative outcomes were achieved for e=20mm, as classified in Table 7 and graphically depicted by the bar chart in Fig. 13.

Table 6. Bearing capacity factors for 2, 3 and 4 layers of geogrid when e=0

	Bearing Capacity Factor (BCF) for e=0											
	x=120mm			x=90mm			x=60mm			x=30mm		
	N=2	N=3	N=4	N=2	N=3	N=4	N=2	N=3	N=4	N=2	N=3	N=4
z/b = 1.0	1.428	1.650	1.739	1.791	2.174	2.555	2.317	2.444	2.870	3.158	3.302	3.462
z/b = 0.75	1.742	1.904	1.974	2.085	2.555	3.031	2.396	2.825	3.136	3.238	3.610	3.983
z/b = 0.50	1.904	1.968	2.151	2.322	2.634	3.158	3.126	3.730	4.2	3.841	4.095	4.526
z/b = 0.25	1.984	2.269	2.460	2.853	3.142	4.079	3.428	4.142	5.333	3.873	5.825	6.476

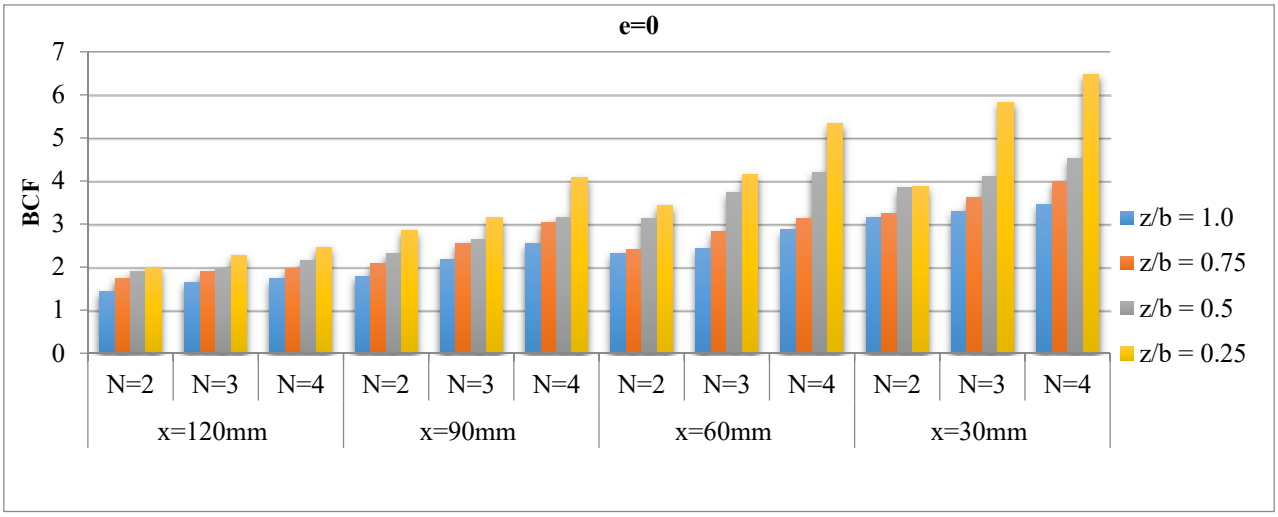

Figure (12): Bearing capacity factors for 2, 3 and 4 layers of geogrid when e= 0

Table 7. Bearing capacity factors for 2, 3 and 4 layers of geogrid when e=20mm

	Bearing Capacity Factor (BCF) for e=20 mm											
	x=120mm			x=90mm			x=60mm			x=30mm		
	N=2	N=3	N=4	N=2	N=3	N=4	N=2	N=3	N=4	N=2	N=3	N=4
z/b = 1.0	1.473	2.263	2.369	1.848	2.657	2.789	2.441	2.789	3.470	3.605	3.963	4.320
z/b = 0.75	1.945	2.447	2.679	2.397	2.896	3.000	3.028	3.473	4.033	4.368	4.770	5.177
z/b = 0.50	2.252	2.578	3.038	2.993	3.399	4.331	3.578	4.263	4.673	4.447	5.710	6.407
z/b = 0.25	2.947	3.225	3.557	3.473	3.941	4.623	3.868	4.447	6.210	4.789	7.763	9.631

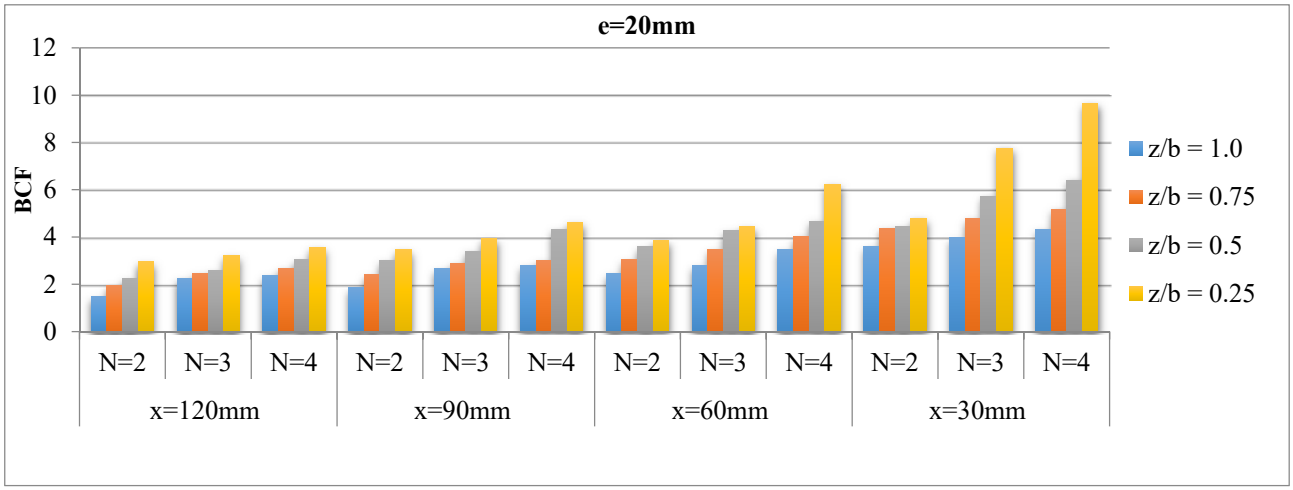

Figure (13): Bearing capacity factors for 2, 3 and 4 layers of geogrid when e= 20 mm

Effect of Load Eccentricity on Bearing Capacity

The effect of load eccentricity has been researched for both strengthened soil and unreinforced soil. The outcomes got plainly show that the bearing capacity of footing reduces with an increase in load eccentricity, for unreinforced soil as well as for geogrid fortified soil. In order to prevent tension in the cross-section and by considering the kern boundary, the maximum limited eccentricity of 20mm has been used in the study.

When the footing is subjected to eccentric load at 20mm, the ultimate load capacity was 39.68% reduced, as compared to that of footing subjected to central load

for unreinforced soil. For geogrid-reinforced soil, the comparative analysis of maximum load intensity subjected to central load and eccentric load has been made and the concluding graph is shown in Fig. 14.

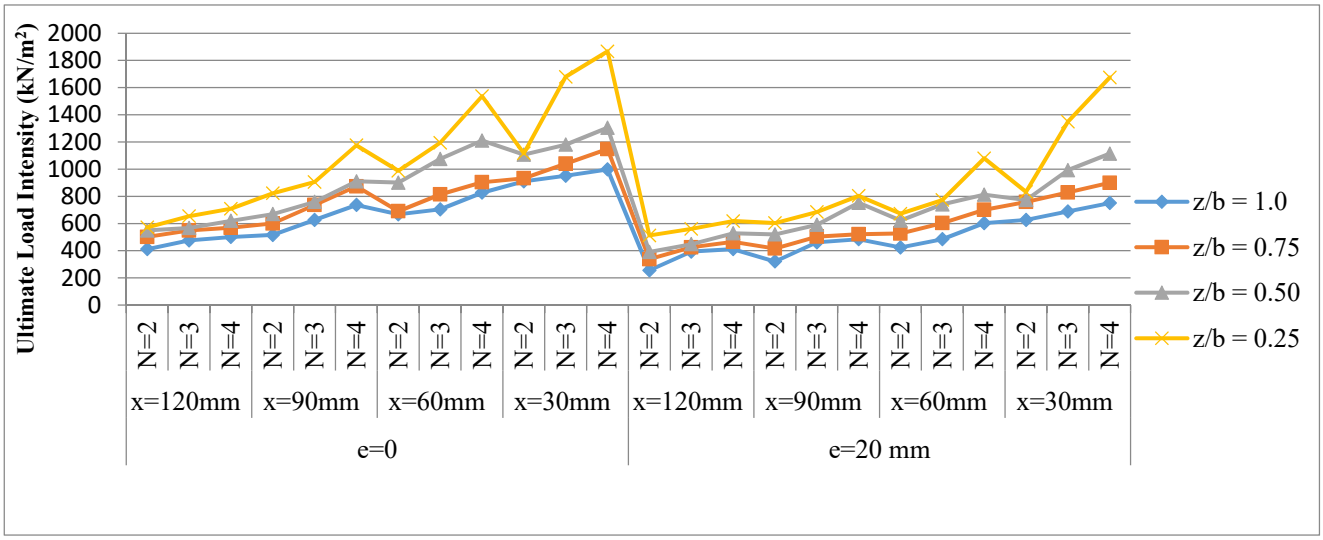

Figure (14): Ultimate load intensities for 2, 3 and 4 layers of geogrid at e=0 and e=20mm

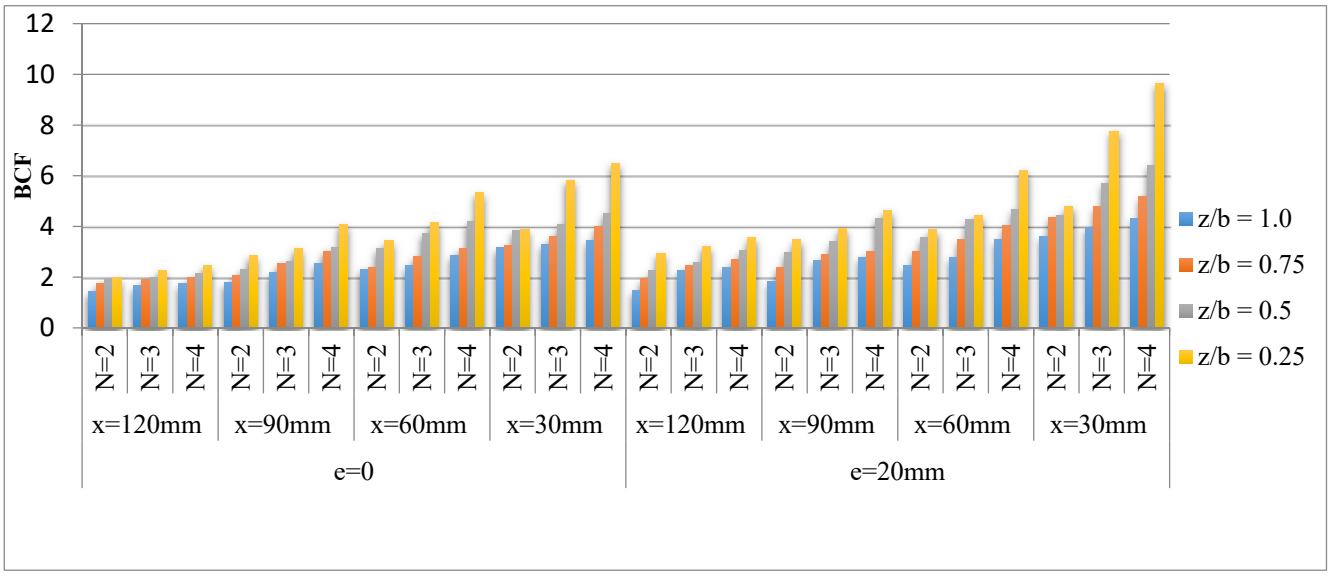

Figure (15): Bearing capacity factors for 2, 3 and 4 layers of geogrid at e=0 and e= 20 mm

For each spacing between geogrid layers having depth ratio z/b=1.0, z/b=0.75, z/b=0.50 and z/b=0.25, maximum load pressure for e=20mm is on average 25.24% less than that for e=0. BCF in all cases has been computed and graphically presented in Fig 15. Bar charts are compared by calculating BCF and it was observed that BCF for eccentric load at 20mm was 23.93% more as compared to BCF calculated for central load.

CONCLUSIONS

A total of 104 laboratory model tests were performed and the ultimate load response of a square footing on unreinforced and geogrid-reinforced sand has been observed when the footing is subjected to central load and eccentric load. The following conclusions are noted in this research area.

1. The use of geosynthetic reinforcement in soil significantly increases the bearing capacity of the soil.
2. The top layer depth of geogrid has been found at a distance of 0.25 times the footing width, from the base of footing for both eccentric and axial load, to accomplish the maximum benefit of geosynthetic reinforcement.
3. The ultimate load intensity has been observed to have its maximum value for a depth ratio of z/b=0.25.
4. BCF rises with increases in the reinforcement layer count up to 4. The BCF for x/b = 0.25 and z/b = 0.25 reaches its highest value in both central and eccentric loads.
5. As the number of layers of geogrid increases from N=2 to N=4, the ultimate load intensities increase, for both e=0 and e=20mm.
6. The BCF for e=20mm is more than the BCF calculated for central load on the footing.
7. The load-carrying capacity of eccentrically loaded footing in the unreinforced case is 39% less than that of footing with central load and for geogrid reinforced sand, it is about 25% less than that of footing subjected to axial load.

REFERENCES

Alawaji, H.A. (2001). “Settlement and bearing capacity of geo-grid-reinforced sand over collapsible soil". Geotextiles and Geomembranes, 19 (2), 75-88.

Aldaood, A., Khalil, A., and Alkiki, I. (2020). "Impact of randomly distributed hay fibers on engineering properties of clay soil." Jordan Journal of Civil Engineering, 14 (3), 406-416.

Das, B.M., and Omar, M.T. (1994). “The effects of foundation width on model tests for the bearing capacity of sand with geo-grid reinforcement". Geotechnical and Geological Engineering, 12 (2), 133-141.

Dash, S.K., Krishnaswamy, N.R., and Rajagopal, K. (2001). “Bearing capacity of strip footings supported on geocell-reinforced sand”. Geotextiles and Geomembranes, 19 (4), 235-256.

Dastpak, P., Abrishami, S., Sharifi, S., and Tabaroei, A. (2020). “Experimental study on the behavior of eccentrically loaded circular footing model resting on reinforced sand”. Geotextile and Geomembranes, March 2020.

Deb, K., and Konai, S. (2014). “Bearing capacity of geotextile-reinforced sand with varying fine fraction”. Geomechanics and Engineering, 6 (1), 33-45.

Durga Prasad, B., Hariprasad, C., and Umashankar, B. (2016). “Load-settlement response of square footing on geogrid-reinforced layered granular beds". International Journal of Geosynthetic & Ground Engineering, 2 (4), 1-10.

Kodicherla, S.P.K., Muktinuthalapati, J., and Revanna, N. (2018). "Effect of randomly distributed fiber reinforcements on engineering properties of beach sand". Jordan Journal of Civil Engineering, 12 (1), 99-108.

Kolay, P.K., Kumar, S., and Tiwari, D. (2013). "Improvement of bearing capacity of shallow foundation on geogrid-reinforced silty clay and sand”. Journal of Construction Engineering, 2013, 1-10.

Makkar, F.M., Chandrakaran, S., and Sankar, N. (2017). “Behaviour of model square footing resting on sand reinforced with three-dimensional geo-grid". International Journal of Geosynthetics and Ground Engineering, 3 (1), 1-10.

Marto, A., Oghabi, M., and Eisazadeh, A. (2013). "Effect of geocell reinforcement in sand and its effect on the bearing capacity with an experimental test: A review". Electronic Journal of Geotechnical Engineering, 18 Q, 3501-3516.

Mirzaeifar, H., and Ghazavi, M. (2015). “Bearing capacity of multi-edge shallow foundations on geogrid-reinforced sand”. The 4th International Conference on Geotechnical Engineering and Soil Mechanics, December 2015.

Mittal, A., and Shukla, S. (2020). "Effect of geogrid reinforcement on the strength, thickness and cost of low-volume rural roads." Jordan Journal of Civil Engineering, 14 (4), 587-597.

Panigrahi, B., and Pradhan, P.K. (2019). “Improvement of bearing capacity of soil by using natural geotextile”. International Journal of GeoEngineering, 10 (1), 1-12.

Patel, S.K., and Singh B. (2017). "Experimental investigation on the behaviour of glass fibre-reinforced cohesive soil for application as pavement subgrade material". International Journal of Geosynthetics and Ground Engineering, 3 (2), 1-12.

Sridhar, R., and Prathapkumar, M.T. (2017). "Behaviour of model footing resting on sand reinforced with a number of layers of coir geotextile". Innovative Infrastructure Solution, 2 (1), 1-8.

Tavangar Y., and Shooshpasha, I. (2016). "Experimental and numerical study of bearing capacity and effect of specimen size on uniform sand with medium density, reinforced with nonwoven geotextile". Arabain Journal of Science and Engineering, 41 (10), 4127-4137.

Zidan, A.F. (2012). "Numerical study of behavior of circular footing on geogrid-reinforced sand under static and dynamic loading". Geotechnical and Geological Engineering, 30 (2), 499-510.